


A wire waveguide channel for terabit-per-second links F

Cite as: Appl. Phys. Lett. **116**, 131102 (2020); <https://doi.org/10.1063/1.5143699>

Submitted: 07 January 2020 . Accepted: 01 March 2020 . Published Online: 31 March 2020

Rabi Shrestha, Kenneth Kerpez, Chan Soo Hwang, Mehdi Mohseni, John M. Cioffi, and Daniel M. Mittleman 

COLLECTIONS

F This paper was selected as Featured



View Online



Export Citation



CrossMark

Lock-in Amplifiers
Find out more today



 Zurich Instruments



A wire waveguide channel for terabit-per-second links

Cite as: Appl. Phys. Lett. **116**, 131102 (2020); doi: [10.1063/1.5143699](https://doi.org/10.1063/1.5143699)

Submitted: 7 January 2020 · Accepted: 1 March 2020 ·

Published Online: 31 March 2020



View Online



Export Citation



CrossMark

Rabi Shrestha,¹ Kenneth Kerpez,² Chan Soo Hwang,² Mehdi Mohseni,² John M. Cioffi,² and Daniel M. Mittleman^{1,a)} 

AFFILIATIONS

¹School of Engineering, Brown University, 184 Hope St, Providence, Rhode Island 02912, USA

²ASSIA, Inc., 203 Redwood Shores Parkway, Suite 100, Redwood City, California 94065, USA

^{a)}Author to whom correspondence should be addressed: daniel_mittleman@brown.edu

ABSTRACT

The rise in consumer data usage has increased the demand for higher data rates in telecommunication in both wireless and wired systems. In order to meet the demands for increased data rates for wired services, one possibility is to switch to higher frequencies, beyond the MHz-range frequencies typically used in digital subscriber line (DSL) services. In this work, we investigate the channel properties of a 200 GHz signal transmitted through a waveguide structure that is designed to approximately emulate the type of paired phone cable typically used for DSL transmissions. We report the attenuation characteristics of such a channel and explore the achievable data rates of a realistic vectored scenario that exploits the modal diversity of this multi-mode channel. We find that aggregate data rates on the order of terabits per second are feasible over short distances.

Published under license by AIP Publishing. <https://doi.org/10.1063/1.5143699>

As the demand increases for higher data rates in both wired and wireless systems, dramatic steps will be necessary for technology to keep pace.¹ Affordable wired services with high data rates have proven to be valuable in managing the bottleneck caused by multiple devices connected to a wireless network. The implementation of digital subscriber line (DSL) services using pre-existing twisted-pair telephone cables offers a unique and effective solution, as these channels can support high data rates, using Discrete Multitone (DMT) modulation with carrier frequencies in the MHz range.² Through ongoing advances in vectoring algorithms and the inclusion of time-domain duplexing, increased achievable downstream rates can reach up to 100 Mbps at a 500 m propagation range, with rates exceeding 1 Gbps attainable at shorter distances.³ These systems often have a significant advantage over fiber optics in their much lower infrastructure costs.²

Recent advances in systems and components for accessing even higher frequencies^{1,4} have opened up the new possibility of exploiting millimeter-wave or terahertz signals in a similar fashion.⁵ A multiplexed twisted-pair copper cable bundle could, in principle, be used as a multi-mode waveguide for high frequencies, exploiting the millimeter-scale air or dielectric gaps between the metal cores as complex waveguides. By exploiting the same sort of vector coding used at lower frequencies in more traditional DSL systems, together with the vastly larger bandwidth available at higher frequencies, a terabit-scale data transmission system could be feasible.

Here, we explore the possibility of using a highly multi-mode waveguiding structure for vectored DSL-type data transmission. To model the fundamental characteristics of such a waveguide, we construct a simplified version of the channel. We use a two-wire waveguide, with an outer metal sheath, which is designed to enclose the energy and eliminate bending losses and simulates the multi-wire twisted-pair phone cables that are often ensheathed in a metallic shield. The two-wire waveguide replicates the behavior of the twisted wire pairs found in cables, and the metallic sheath replicates the external metallic conduit or alternatively the outermost set of twisted-pairs that can effectively act as a solid sheath for millimeter waves. A bare two-wire system is a well-known waveguide structure that has been shown to guide THz waves efficiently. In the TEM mode, this waveguide experiences only moderate radiation losses upon bending.^{6,7} The addition of an external metallic sheath essentially eliminates these bending losses at the expense of additional Ohmic losses in the metal, as radiating energy is reflected and confined within the structure, recoupling back onto the waveguide, although, obviously, with significant mode mixing. This mode mixing is, in our case, an advantage: just as in wireless systems, where multi-path scattering leads to a rich channel for multiple orthogonal data streams,⁸ the multiple modes of a complicated waveguiding structure lead to the possibility of orthogonal data channels in this guided-wave structure.⁹

The channel used for the experiments in this work consists of a two-wire waveguide inside a stainless-steel sheath (see the inset of Fig. 1). The waveguide consists of two copper wires of 0.5 mm diameter (the most common gauge used in a telephone cable) separated vertically by 1 mm (center to center distance), approximately centered within a 12.5 mm diameter outer metallic pipe which acts as the sheath. The two wires are kept parallel throughout the length of the entire structure by small Teflon holders located at periodic intervals inside the sheath. The waveguide includes a single bend of 32.3° near the input end followed by a straight section of variable length. The bend induces significant mode mixing among the various waveguide modes that are launched at the input, because of the recoupling mechanism mentioned above. This bend also prevents any direct line-of-sight free-space coupling between the transmitter and receiver that could confuse the measurement results.

Our transmitter consists of a frequency multiplier chain (Virginia Diodes) producing a continuous 200 GHz signal with a power of approximately 20 dBm and vertical polarization. This signal is coupled into free space using a conical horn antenna. This free-space beam is then focused quasi-optically using dielectric lenses to a roughly diffraction-limited spot at the input plane of the sheath/two-wire structure. This focal point is an approximately Gaussian spot (about 1 mm diameter), which is small compared to the size of the sheath's input aperture (Fig. 2). As a result, the superposition of modes that are initially excited is, in general, quite complex, and also quite sensitive to the location of this input illumination spot relative to the structure. After this excitation propagates past the bend, the resulting mode structure is mixed even further, resulting in an essentially chaotic mode pattern. At the output end of the structure, we characterize this complex mode by spatially resolving the output.¹⁰ This is accomplished using a 1 mm diameter aperture to isolate only a portion of the output, followed by a horn antenna coupled to a zero-bias Schottky diode receiver (Virginia Diodes) for detection of the received power.¹¹ For a given location of the illuminated spot on the input face, we measure the output power at all points in a $13\text{-mm} \times 13\text{-mm}$ grid, using a motorized pair of translation stages to scan the location of the receiver and aperture sequentially through all locations. This range of receiver positions covers the entire region of the output plane of the guiding structure that is contained within the metallic sheath (6.5 mm displacement from the center of the two-wire waveguide in both transverse

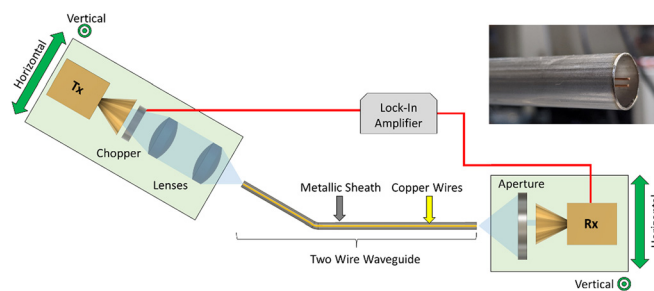


FIG. 1. Top view of the experimental setup for measuring the spatial profile of power in the multi-mode waveguide described in the text. Both the input excitation spot (Tx) and the output measurement location (Rx) can be scanned in two dimensions (horizontal and vertical, as labeled), in a plane perpendicular to the waveguide propagation axis. Inset: A photograph of the input of the waveguide.

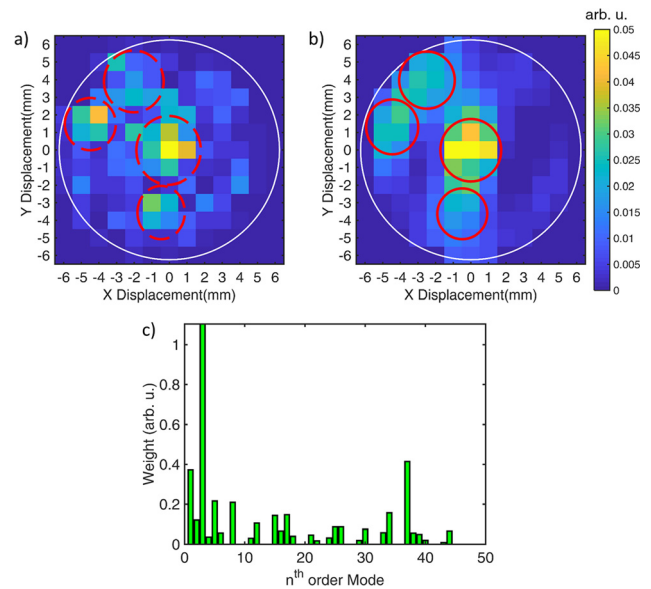


FIG. 2. (a) Measured and (b) simulated output of the waveguide when the input excitation location is symmetrically located between the two copper wires. The red circles highlight similar patterns present in both spatial profiles. The simulation includes the 50 lowest-order eigenmodes of the composite waveguide structure. (c) The distributed weights for the eigenmodes extracted from the mode simulation.

directions), so this procedure forms an image of the spatial distribution of the power in the output plane.

Figure 2(a) illustrates one typical result for a total length of 37 cm. This shows the output power distribution for one particular input illumination spot. In this case, the input spot corresponds to the location directly centered on the two-wire structure. This location is the one that is most likely to excite a small number of propagating modes at the input port—indeed, an ideal mode matching at this location would excite the TEM waveguide mode of the two-wire structure with 52% coupling efficiency. Yet, even in this case, it is obvious that the output spatial profile does not resemble the TEM mode (or any other low-order mode) of a two-wire waveguide.^{6,12} The presence of multiple maxima in the spatial profile (circled in red) demonstrates the presence of multimode mixing in the channel, which likely originates from the bend, as well as other unintentional inhomogeneities in the separation and parallelism of the two wires. In the context of DSL-style data transmission, we interpret this multimode mixing in analogy to the rich multi-path scattering that is crucial for achieving MIMO gain in wireless systems.⁸

We investigate the degree of mode mixing using a numerical decomposition of the measured profile in Fig. 2(a). Using the modes of the structure that are computed numerically via finite element analysis (COMSOL), accounting for both the two wires and the metal sheath, the simulations approximately reproduce the measured spatial profile, as shown in Fig. 2(b). Obviously, the accuracy of the decomposition is limited by the number of modes used in the reconstruction; in this example, we employ the lowest 50 modes of the structure to illustrate the degree of mode mixing that is typical in our measurements [Fig. 2(c)]. Even for the relatively higher-order modes in this superposition, the waveguide remains significantly over-moded, which limits the effects of modal dispersion on the output signal.⁹

A full characterization of the channel requires a measurement of the output profile [e.g., Fig. 2(a)] for all possible input excitation conditions. Therefore, we repeat the imaging procedure described above for all possible positions of the illumination spot on the input plane (on a 13-mm \times 13-mm grid). The resulting 169×169 matrix represents a complete input-output characterization of the channel's amplitude response. This data set is summarized in Fig. 3. Furthermore, to investigate how the channel properties depend on the length of the waveguide, we repeat this full set of measurements for several different waveguide lengths (67, 102, 137, and 177 cm total length). For all these measurements, the portion of the waveguide prior to and including the bend remains fixed; only the length of the straight section following the bend is changed. This procedure is equivalent to a "cut-back" measurement of waveguide output vs length, which enables a quantitative estimate of the overall loss, as discussed below.

In the case of a rich multi-mode waveguide, one can envision taking advantage of multimode mixing by implementing vectoring techniques, essentially equivalent to a MIMO configuration in wireless systems, which increases the overall channel capacity in proportion to the number of transmitter and receiver antennas. Each of the subchannels are eigenmodes of the channel and are traditionally exploited with multiple transmitters and receivers operating in parallel. In our case, we can explore this possibility using the measured 169×169 data matrix that connects all possible transmitter locations to all possible receiver locations. Our experimental capability is limited to a single transmitter and a single receiver; however, the measured matrix is sufficient to demonstrate that the necessary mode mixing is present even in this simplified model of a twisted-pair cable, and also to simulate the operation of a vectored system with multiple transmitters and receivers.

From the data of Fig. 3, we compute the singular values of the channel matrix between the transmitter and receiver. Since the waveguide exhibits the properties of a channel with a rich diversity, we obtain a full non-zero set of singular values for the matrix. From these

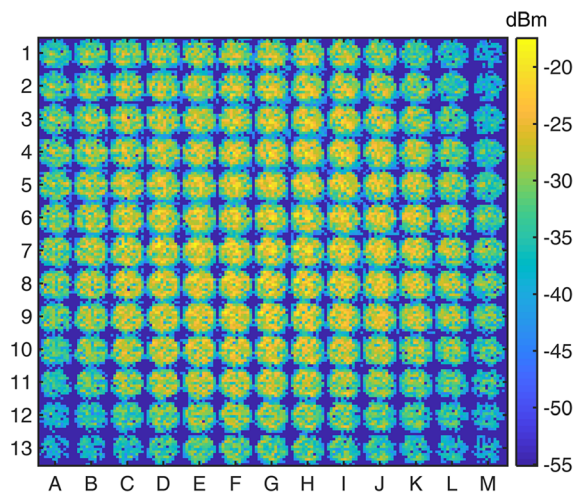


FIG. 3. The complete input-output 169×169 channel matrix for the waveguide structure, connecting all possible input excitation locations to all possible output measurement locations. For these measurements, both the input and output facets are subdivided into 13×13 grids of 1 mm^2 size (i.e., when the input is focused into the waveguide at location G9, we measure a spatial profile at the output corresponding to the same grid position in Fig. 3).

values, we can calculate an achievable aggregate data rate, using some realistic assumptions about the number of independent transmitters and receivers. We may assume, for example, a system with eight independent broadband transmitters and receivers, all accessing the same channel matrix (i.e., Fig. 3). This assumption is only a mild extrapolation from existing CMOS-based transceiver architectures.^{13,14} Our simulation uses only the 8 largest singular values, and assumes DMT modulation with bit-loading up to 12 bits/Hz centered at 200 GHz (our measurement frequency). We calculate the maximum achievable data rate from $C = B \sum_j \log_2(1 + \text{SNR} \cdot \sigma_j / \Gamma)$ on each of the 2048 subcarriers, and sum the data rate across all subcarriers. Here, SNR is the signal-to-noise ratio, assuming a transmit power of 15 dBm per transmitter and a noise floor of -160 dBm/Hz ,¹⁵ σ_j is the square of the j th singular value, and B is the accessible bandwidth. Γ is the coding gap, about 9.75 dB for QAM.¹⁶ We assume a bandwidth of 200 GHz, consistent with that which can presently be achieved in integrated devices.¹⁷

One key parameter in this calculation is the achievable signal-to-noise ratio. To accurately assess this value, we must account for attenuation in the waveguide resulting from the finite conductivity of the metal components. This loss is different for different waveguide modes and is, therefore, difficult to predict because of the complex nature of the mode mixing. A rough estimate of the attenuation for a given propagation length can be obtained using the analytical expression for the loss of the TE_{mn} mode of a metal waveguide of circular cross section (radius a),

$$(\alpha_c)_{mn}^{\text{TE}} = \frac{8.686 R_s}{a \eta \sqrt{1 - (f_c/f)^2}} \left[\left(\frac{f_c}{f} \right)^2 + \frac{m^2}{(\chi'_{mn})^2 - m^2} \right]. \quad (1)$$

In this expression, χ'_{mn} are the n th zeros of the m th-order derivative of the Bessel function, f_c is the cutoff frequency, η is the wave

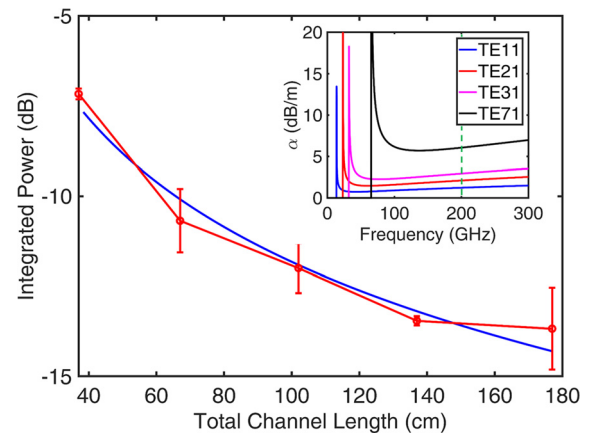


FIG. 4. Measured and numerically estimated total output power as a function of the length of the waveguide structure. The numerical calculation includes only a single fit parameter, which is an overall multiplicative scaling constant representing the total power coupled into the input end of the waveguide. The nonlinear behavior is due to the fact that higher-order modes contained in the multi-mode superposition decay much more rapidly at a given frequency due to higher Ohmic losses. Inset: Ohmic loss for several TE_{mn} modes of a circular pipe waveguide, from Eq. (1). The vertical dashed line at 200 GHz indicates the operating frequency of the measurements described here.

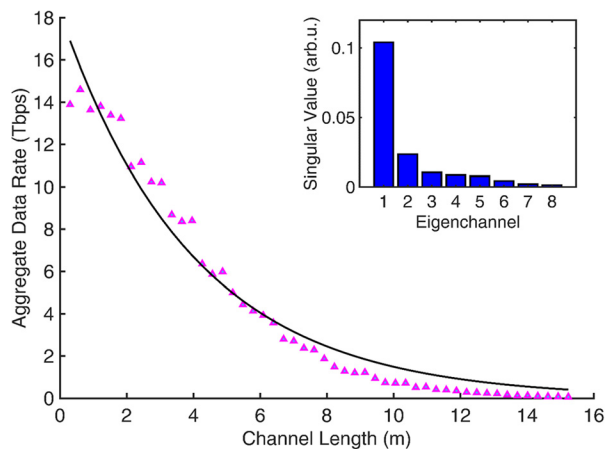


FIG. 5. The calculated aggregate data rate as a function of the channel length, using the assumptions described in the text. High data rates in the Tbps range are achievable at short distances, dropping to about 30 Gbps at 15 m. Inset: The eight largest singular values of the channel matrix shown in Fig. 3.

impedance, R_s is the sheet resistance of the metal, and the result is obtained in dB/m.¹⁸ This estimate assumes that the eigenmodes of our waveguides are equivalent to those of a hollow metal pipe, and therefore ignores the effects of the metal wires contained within the sheath. This is a reasonable approximation, since the copper wires only contribute a small additional amount to the total exposed metal surface area, and therefore should have a relatively small impact on the Ohmic losses.

In order to make a comparison to our measurements of the wave attenuation, we assume that the propagating wave consists of a superposition of the lowest 14 TE modes, each of which attenuates according to Eq. (1) with the weighting coefficients of each mode extracted from the simulation [Fig. 2(c)]. We then compute the total power in the electromagnetic wave as a function of the propagation distance.¹⁹ This result is shown as the solid curve in Fig. 4, along with the measured power levels, which are obtained by integrating the total power in a spatially resolved image of the output facet [such as the one shown in Fig. 2(a)]. The reasonable correspondence between the measurements and this model calculation suggests that the attenuation is indeed dominated by Ohmic waveguide losses, mainly in the metallic sheath. We therefore use this approach to estimate the signal-to-noise, and therefore the channel capacity, as a function of the length of the structure. The data rates predicted in this way are shown in Fig. 5. We predict a high data rate of several terabits per second (Tbps) at short distances of a few meters, dropping to 30 Gbps at a range of 15 m. Thus, this parallelized multi-mode waveguide approach can provide

extremely high capacity for data transmission over short and moderate distances.

In summary, we have demonstrated a MIMO link for a two-wire channel capable of supporting data rates exceeding Tbps. We have shown that the channel is limited in range by the Ohmic loss from the surface of the metallic sheath. Such a transmission system may be ideally suited for situations that demand very high data rates over a relatively short range, such as in data centers or for chip-to-chip connections. Extending the system to a larger range would require reducing the Ohmic loss of the system, which will require further investigation.

We would like to acknowledge the support provided by the U.S. National Science Foundation.

REFERENCES

- ¹K. Sengupta, T. Nagatsuma, and D. M. Mittleman, *Nat. Electron.* **1**, 622–635 (2018).
- ²J. M. Cioffi, S. Jagannathan, M. Mohseni, and G. Ginis, *IEEE Commun. Mag.* **45**, 132–139 (2007).
- ³M. Wolderstorfer and D. Statovci, in *IEEE Symposium on Signal Processing and Information Technology* (Bilbao, Spain, 2017), pp. 83–88.
- ⁴J. Federici and L. Moeller, *J. Appl. Phys.* **107**, 111101 (2010).
- ⁵J. M. Cioffi, K. J. Kerpez, C. S. Hwang, and I. Kanellakopoulos, *IEEE Commun. Mag.* **56**, 152–159 (2018).
- ⁶M. Mbonye, R. Mendis, and D. M. Mittleman, *Appl. Phys. Lett.* **95**, 233506 (2009).
- ⁷V. Astley, J. Scheiman, R. Mendis, and D. M. Mittleman, *Opt. Lett.* **35**, 553–555 (2010).
- ⁸O. Souihli and T. Ohtsuki, *IEEE Commun. Lett.* **17**, 23–26 (2013).
- ⁹X. Chen, J. He, A. Li, J. Ye, and W. Shieh, *IEEE Photonics Tech. Lett.* **25**, 1819–1822 (2013).
- ¹⁰H. Zhan, R. Mendis, and D. M. Mittleman, *J. Opt. Soc. Am. B* **28**, 558–566 (2011).
- ¹¹Y. Amarasinghe, D. M. Mittleman, and R. Mendis, *J. Infrared, Millimeter, Terahertz Waves* **40**, 1129–1136 (2019).
- ¹²H. Pahlavaninezhad, T. E. Darcie, and B. Heshmat, *Opt. Express* **18**, 7415–7420 (2010).
- ¹³M. Sawaby, N. Dolatsha, B. Grave, C. Chen, and A. Arbabian, *IEEE Solid-State Circuits Lett.* **1**, 166–169 (2018).
- ¹⁴K. Katayama, K. Takano, S. Amakawa, S. Hara, A. Kasamatsu, K. Mizuno, K. Takahashi, T. Yoshida, and M. Fujishima, *IEEE J. Solid-State Circuits* **51**, 3037–3048 (2016).
- ¹⁵X. Wu and K. Sengupta, *Opt. Express* **26**, 7163–7175 (2018).
- ¹⁶I. Otung, *Digital Communications: Principles and Systems* (Institution of Engineering and Technology, London, 2014).
- ¹⁷T. Chi, M.-Y. Huang, S. Li, and H. Wang, in *IEEE International Solid-State Circuits Conference (ISSCC)* (San Francisco, 2017), pp. 304–305.
- ¹⁸C. A. Balanis, *Advanced Engineering Electromagnetics*, 2nd ed. (John Wiley & Sons, 2012).
- ¹⁹S. Ramo, T. Van Duzer, and J. R. Whinnery, *Fields and Waves in Communication Electronics*, 3rd ed. (John Wiley & Sons, 1994).